

Methodology for Production Data Integration by Numerical Calculation of Sensitivity Coefficients

Linan Zhang¹, Thies Dose², Clayton V. Deutsch¹, and Luciane Cunha¹

¹Civil & Environmental Engineering
University of Alberta

²RWE-DEA Aktiengesellschaft

Abstract

This paper is the first part in a three-part series that presents a methodology for production data integration in large reservoirs with long production/injection history. There is a need for practical techniques for production data integration in realistic reservoir models. A methodology is proposed to integrate production data into reservoir models by the local updating of porosity and permeability fields. The focus is on conditioning an initial model to injection/production rate and pressure history in an iterative fashion. The sequential self calibration (SSC) methodology is extended to be used with a commercial simulator and numerical calculation of sensitivity coefficients. This method makes it possible to condition the permeability/porosity distributions to historical injection/production rate and pressure historical data from large reservoirs with complex heterogeneity and complex changes in the production history.

Introduction

Optimal reservoir management requires reliable reservoir performance forecasts with as little uncertainty as possible. These production forecasts are directly related to the reservoir size and internal porous media properties. Dynamic production data contain important information about reservoir structure and petrophysical properties. Any reliable reservoir characterization study should account for the available deemed reliable production data.

Many researchers have worked on production data integration and several methods have been proposed. A challenge remains in the conditioning of reservoir property models to production data in large scale fields with a long production/injection history. Direct calculation schemes are avoided considering that they are often limited to 2-D single-phase flow. Stochastic approaches such as simulated annealing or genetic algorithms^[1,2] require excessive run time. Publicly available sequential self calibration^[3,4] algorithms are difficult to adapt to complex reservoir conditions with changing well conditions and multiphase flow. Streamline simulation methods are being adapted to multiphase flow^[5-7]; however, they require a custom-written simulator that is inherently limited in flexibility. The convergence of gradual deformation methods is slow in presence of large 3-D models^[8,9]. Regularization methods such as Bayesian based techniques can lower the uncertainty of the property models conditional to historical production data but they need reliable prior information that is difficult to guarantee in many cases^[10].

Well bottom-hole pressure and production rate data are obtained intermittently during the reservoir production. These data are highly depended on the underlying distribution of rock and fluid properties. There are a number of considerations for a practical technique to integrate these data in practical reservoir modeling: (1) the number of full-field flow simulations must be limited,

(2) multiphase flow and the complex changes in well conditions must be handled, and (3) sensitivity coefficients or some accelerated inversion scheme must be considered.

Historical production data are often integrated in geostatistical reservoir modeling by history matching, which often requires many flow simulations. This is time consuming for large 3-D models. Gradual Deformation Method (GDM) was used in a real field case located offshore Brazil and about 100 simulations are required^[8]. Stochastic approaches often need thousands of flow simulation runs^[1,2]. Flow simulation is often used at each iteration to check the goodness of the updated models.

Multiphase flow and complex changes in well conditions are problematic for most production data integration algorithms. An important feature of virtually all production data integration algorithms is the requirement to calculate the sensitivity of well bottom hole pressure and fractional flow rate subject to changes in the porosity and permeability. Analytical methods including streamline-based methods are difficult to adapt to complex multiphase flow and frequent complex well changes. There has been some limited success with streamline and analytical methods, but concerns remain^[11,12].

There is a need for a novel computational efficient production data integration method that: (1) integrates well bottom pressure and production rate simultaneously by limited flow simulation runs, and (2) maintains practicality in large complex 3-D reservoir models with high heterogeneous property models, multiple phases, complex well system change and long history of production and injection. Our effort aims at developing an integration method that builds on commercially available flow simulators (Eclipse in this case) and trades off from previous production data integration methods. The status of our efforts is shown in a three-part series of papers. This is the first part.

Basic Idea and General Procedure of the Proposed Methodology

Our basic idea consists of using the sequential self calibration (SSC) scheme with 5-20 main outer iterations to achieve convergence. The sensitivity coefficients, however, are calculated numerically on the basis of two flow simulations – the preceding flow simulation and a customized changed realization. The difficult analytical calculation of the sensitivity coefficients is replaced by a simpler algorithm. The approximate sensitivity coefficients are then used to locally update the property models. It is important to note that we do *not* perform a perturbed flow simulation for each sensitivity coefficient. We perform only one additional flow simulation and approximatively infer all of the sensitivity coefficients. The procedure is iterated until the results are satisfied or can not be improved. A flowchart of the proposed methodology is shown in Figure 1.

The initial geostatistical realization reproduces all of the static data possible. This is used in the commercial flow simulator to calculate the mismatch in pressure and fractional flow rate between simulation results and historical data. One or more perturbation locations are chosen based on the local mismatch at well locations – areas with greater mismatch are given a greater probability of being chosen for perturbation. The porosity and permeability are drastically changed by a factor of 0.5 or 1.5 at the chosen locations. Those drastic changes are propagated to the entire grid. A second flow simulation with the perturbed model is performed and the numerical sensitivity coefficients are calculated. The optimal changes to the reservoir properties can be calculated by a linear approximation to the flow equations. Note that the drastically changed model is only used for the inference of sensitivity coefficients. The optimal changes are propagated to the entire grid

system. This procedure can be iterated. Past experience with this overall SSC scheme and experience with the proposed scheme indicates that most improvements are in the first 5-10 iterations. A further 10 iterations may be warranted. Figure 2 gives an example. There are 2 full field flow simulations per iteration.

The simulation runs could be performed with any simulator; however, we use the ECLIPSE flow simulator^[13]. This allows the consideration of complex geometry and heterogeneity of reservoir models as well as realistic well scheduling.

Two main features distinguish this method from others: (1) numerically calculated sensitivity coefficients with linearized formula of reservoir behavior and (2) the flexibility to handle any structure, flow regime and well conditions.

Some Details of the Proposed Methodology

The pore volume and permeability of the input initial models will be changed in areas that are “tested” by the available production data. The main steps will be discussed below. Historical data of well bottom-hole pressure and fractional flow rate measurements at all well locations are denoted:

$$p_{w,t}, \text{ for } w=1, 2, \dots, n_w \text{ and } t=1, 2, \dots, n_{w,p}$$

$$q_{w,t}, \text{ for } w=1, 2, \dots, n_w \text{ and } t=1, 2, \dots, n_{w,q}$$

Each well has a different number of available pressure and fractional flow rate values:

$$n_{i,p} \neq n_{j,p} \quad (1)$$

$$n_{i,q} \neq n_{j,q} \quad (2)$$

for $i, j=1, 2, \dots, n_w$ and $j \neq i$

The number of available observation points of pressure and fractional flow rate are given by:

$$n_p = \sum_{w=1}^{n_w} n_{w,p} \quad (3)$$

$$n_q = \sum_{w=1}^{n_w} n_{w,q} \quad (4)$$

Often:

$$n_p \neq n_q \quad (5)$$

$$n_w n_{w,p} \neq n_p \quad (6)$$

$$n_w n_{w,q} \neq n_q \quad (7)$$

for $w=1, 2, \dots, n_w$

The initial porosity and permeability realization at all locations is denoted:

$$\phi^0(\mathbf{u}_g), K_h^0(\mathbf{u}_g), K_v^0(\mathbf{u}_g), \text{ for } g=1, 2, \dots, N$$

Step 1: Flow Simulation Run with Initial Model

Here the objective is to run the flow simulator (ECLIPSE) in history matching mode to establish the pressure and fractional flow rate at all well locations for all time corresponding to the historical data:

$$p_{w,t}^0, \text{ for } w=1, 2, \dots, n_w \text{ and } t=1, 2, \dots, n_{w,p}$$

$$q_{w,t}^0, \text{ for } w=1, 2, \dots, n_w \text{ and } t=1, 2, \dots, n_{w,q}$$

Step 2: Mismatch Analysis of the Initial Case

Different wells have different importance and should receive different weights. A weight, β_w is applied to each well. The observed data points are weighted by $\lambda_{w,p,t}$ and $\lambda_{w,q,t}$. The measurements of mismatch in pressure and fractional flow rate are defined as:

$$\Delta P^i = \sum_{w=1}^{n_w} \left\{ \sum_{t=1}^{n_{w,p}} (p_{w,t}^i - p_{w,t})^2 \lambda_{w,p,t} \right\} \beta_w \quad (8)$$

$$\Delta Q^i = \sum_{w=1}^{n_w} \left\{ \sum_{t=1}^{n_{w,q}} (q_{w,t}^i - q_{w,t})^2 \lambda_{w,q,t} \right\} \beta_w \quad (9)$$

For the initial base case:

$$\Delta P^0 = \sum_{w=1}^{n_w} \left\{ \sum_{t=1}^{n_{w,p}} (p_{w,t}^0 - p_{w,t})^2 \lambda_{w,p,t} \right\} \beta_w \quad (10)$$

$$\Delta Q^0 = \sum_{w=1}^{n_w} \left\{ \sum_{t=1}^{n_{w,q}} (q_{w,t}^0 - q_{w,t})^2 \lambda_{w,q,t} \right\} \beta_w \quad (11)$$

Mismatch in pressure and fractional flow rates for each well can be calculated by:

$$\Delta P_w^i = \sum_{t=1}^{n_{w,p}} (p_{w,t}^i - p_{w,t})^2 \lambda_{w,p,t} \quad (12)$$

$$\Delta Q_w^i = \sum_{t=1}^{n_{w,q}} (q_{w,t}^i - q_{w,t})^2 \lambda_{w,q,t} \quad (13)$$

for $w=1, 2, \dots, n_w$

The global mismatch for the reservoir is calculated as:

$$\Delta^i = w_p \left(\frac{\Delta P^i}{2\Delta P^0} \right) + w_q \left(\frac{\Delta Q^i}{2\Delta Q^0} \right) \quad (14)$$

The “local” mismatch at each well is calculated using ΔP^0 and ΔQ^0 as global scaling factors:

$$\Delta_w = \beta_w \left\{ w_p \left(\frac{\Delta P_w}{2\Delta P^0} \right) + w_q \left(\frac{\Delta Q_w}{2\Delta Q^0} \right) \right\} \quad (15)$$

for $w=1, 2, \dots, n_w$

where w_p and w_q are weights for mismatch in pressure and fractional flow rates, respectively. In general, $w_p + w_q = 2$. For the base model, $\Delta^0 = 1$.

Step 3: Selection of Perturbation Locations and Propagation of the Perturbations

The perturbation locations, \mathbf{u}_s , $s=1,2,\dots,n_s$, are selected from a 2-D “mismatch” map based on the mismatch at each well. The locations will be near active wells. In general, the perturbations are propagated within a radius approximately equal to the well spacing. Each perturbation is independent of the others. The number and positions of perturbations may be different for each iteration. A schematic plot is shown in Figure 3. There are n_s perturbation locations:

$$\mathbf{u}_s \quad \text{for } s=1,2,\dots, n_s$$

The perturbation factors can be set to 1.5 or 0.5 at perturbation locations:

$$f(\mathbf{u}_s) \quad \text{for } s = 1, 2, \dots, n_s$$

The perturbations are propagated to all grid blocks by simple kriging with mean of 1 and suitable ranges conditioned to the factors at the perturbation locations and assuming that the grid blocks at the same horizontal position but different vertical position have the same perturbation factor:

$$f(\mathbf{u}_g) \quad \text{for } g = 1, 2, \dots, N$$

The perturbations of porosity or permeability can be calculated by the following formulas:

$$\Delta \hat{\phi}^i(\mathbf{u}_g) = \phi^i(\mathbf{u}_g) \cdot (f(\mathbf{u}_g) - 1) \quad (16)$$

$$\Delta \hat{K}_h^i(\mathbf{u}_g) = K_h^i(\mathbf{u}_g) (f(\mathbf{u}_g) - 1) \quad (17)$$

$$\Delta \hat{K}_v^i(\mathbf{u}_g) = K_v^i(\mathbf{u}_g) (f(\mathbf{u}_g) - 1) \quad (18)$$

$$\text{for } g = 1, 2, \dots, N$$

Step 4: Construction of the Perturbed Models

Perturbed property models are created by:

$$\hat{\phi}^i(\mathbf{u}_g) = \phi^i(\mathbf{u}_g) + \Delta \hat{\phi}^i(\mathbf{u}_g) \quad (19)$$

$$\hat{K}_h^i(\mathbf{u}_g) = K_h^i(\mathbf{u}_g) + \Delta \hat{K}_h^i(\mathbf{u}_g) \quad (20)$$

$$\hat{K}_v^i(\mathbf{u}_g) = K_v^i(\mathbf{u}_g) + \Delta \hat{K}_v^i(\mathbf{u}_g) \quad (21)$$

$$\text{for } g = 1, 2, \dots, N$$

Step 5: Rerun Flow Simulation with the Perturbed Models

At this stage a new flow simulation run is executed based on the perturbed models created in Step 4 and a new set of simulation results is obtained:

$$\hat{p}_{w,t} \quad \text{for } w = 1, 2, \dots, n_w \text{ and } t = 1, 2, \dots, n_{w,p}$$

$$\hat{q}_{w,t} \quad \text{for } w = 1, 2, \dots, n_w \text{ and } t = 1, 2, \dots, n_{w,q}$$

Step 6: Calculation of Sensitivity Coefficients and Optimization for Property Changes at Master Point Locations

The number of master point locations is n_m , with $n_m \geq n_s$. The master point locations are:

$$\mathbf{u}_m \quad \text{for } m=1, 2, \dots, n_m$$

For example, if one master point location is selected at each perturbation location, $n_s = n_m$; if three master point locations are selected at each perturbation location, $n_m = 3n_s$. An illustration is shown in Figure 4.

Parameters used to measure the change of mismatch are introduced as:

$$\Delta_P^{2i} = \frac{\Delta P^i - \Delta P^0}{\Delta P^0} \quad (22)$$

$$\Delta_Q^{2i} = \frac{\Delta Q^i - \Delta Q^0}{\Delta Q^0} \quad (23)$$

$$\Delta^{2i} = w_p \left(\frac{\Delta_P^{2i}}{2} \right) + w_q \left(\frac{\Delta_Q^{2i}}{2} \right) \quad (24)$$

where, Δ^{2i} is the objective function that can be used to obtain optimal changes at all master point locations. The pressure and fractional flow rates are only available at well locations. The master point locations are used for the optimization and changed between the iterations because the perturbation locations are changed between iterations.

The sensitivity coefficients at each master point location and each time step corresponding to the observed data are calculated by the following formula:

$$SP_{\phi, m, w, t}^i = \frac{\partial p_{w, t, m}}{\partial \phi(\mathbf{u}_m)} = \frac{\hat{p}_{w, t, m} - p_{w, t}^i}{\Delta \hat{\phi}(\mathbf{u}_m)} = \frac{\Delta p_{w, t, m}^i}{\Delta \hat{\phi}(\mathbf{u}_m)} \quad (25)$$

$$SP_{K_h, m, w, t}^i = \frac{\partial p_{w, t, m}}{\partial K_h(\mathbf{u}_m)} = \frac{\hat{p}_{w, t, m} - p_{w, t}^i}{\Delta \hat{K}_h(\mathbf{u}_m)} = \frac{\Delta p_{w, t, m}^i}{\Delta \hat{K}_h(\mathbf{u}_m)} \quad (26)$$

$$SP_{K_v, m, w, t}^i = \frac{\partial p_{w, t, m}}{\partial K_v(\mathbf{u}_m)} = \frac{\hat{p}_{w, t, m} - p_{w, t}^i}{\Delta \hat{K}_v(\mathbf{u}_m)} = \frac{\Delta p_{w, t, m}^i}{\Delta \hat{K}_v(\mathbf{u}_m)} \quad (27)$$

for $w=1, 2, \dots, n_w$, $t=1, 2, \dots, n_{w,p}$ and $m=1, 2, \dots, n_m$

$$SQ_{\phi, m, w, t}^i = \frac{\partial q_{w, t, m}}{\partial \phi(\mathbf{u}_m)} = \frac{\hat{q}_{w, t, m} - q_{w, t}^i}{\Delta \hat{\phi}(\mathbf{u}_m)} = \frac{\Delta q_{w, t, m}^i}{\Delta \hat{\phi}(\mathbf{u}_m)} \quad (28)$$

$$SQ_{K_h, m, w, t}^i = \frac{\partial q_{w, t, m}}{\partial K_h(\mathbf{u}_m)} = \frac{\hat{q}_{w, t, m} - q_{w, t}^i}{\Delta \hat{K}_h(\mathbf{u}_m)} = \frac{\Delta q_{w, t, m}^i}{\Delta \hat{K}_h(\mathbf{u}_m)} \quad (29)$$

$$SQ_{K_v, m, w, t}^i = \frac{\partial q_{w, t, m}}{\partial K_v(\mathbf{u}_m)} = \frac{\hat{q}_{w, t, m} - q_{w, t}^i}{\Delta \hat{K}_v(\mathbf{u}_m)} = \frac{\Delta q_{w, t, m}^i}{\Delta \hat{K}_v(\mathbf{u}_m)} \quad (30)$$

for $w=1, 2, \dots, n_w$, $t=1, 2, \dots, n_{w, q}$ and $m=1, 2, \dots, n_m$

$\Delta p_{w, t, m}^i$ and $\Delta q_{w, t, m}^i$ refer to the changes of pressure and fractional flow rate introduced by the perturbation at the location \mathbf{u}_m without considering the other perturbations.

For multiple perturbation locations in each iteration, the changes of well bottom hole pressure and oil production rates at all wells are the total effect caused by the joint property changes propagated from the multiple perturbation locations. The difference of pressure and oil production rates between one base simulation and one perturbation simulation, $\Delta p_{w, t, total}$ and $\Delta q_{w, t, total}$, for $w=1, 2, \dots, n_w$, are used to numerically calculate all the necessary sensitivity coefficients. The key to this approach is the decomposition of the changes in pressure and production rates introduced by joint multiple perturbations to generate $\Delta p_{w, t, m}^i$ and $\Delta q_{w, t, m}^i$.

$\Delta p_{w, t, m}^i$ and $\Delta q_{w, t, m}^i$ used in Equations (25) to (30) can be calculated by the changes of pressure and production rates introduced by joint multiple perturbations, $\Delta p_{w, t, total}$ and $\Delta q_{w, t, total}$, for $w=1, 2, \dots, n_w$:

$$\Delta p_{w, t, m}^i \approx \alpha_{w, m} \Delta p_{w, t, total}^i \quad (31)$$

for $w=1, 2, \dots, n_w$, $t=1, 2, \dots, n_{w, p}$ and $m=1, 2, \dots, n_m$

$$\Delta q_{w, t, m}^i \approx \alpha_{w, m} \Delta q_{w, t, total}^i \quad (32)$$

for $w=1, 2, \dots, n_w$, $t=1, 2, \dots, n_{w, q}$ and $m=1, 2, \dots, n_m$

where a modified ‘‘inverse distance method’’^[14] is used to calculate the decomposition weights:

$$\alpha_{w, m} = \frac{\frac{(k_h \cdot h)_m}{(d+c)_m^\omega}}{\sum_i^{n_m} \frac{(k_h \cdot h)_i}{(d+c)_i^\omega}} \quad (33)$$

$(k \cdot h)_m$ is the product of property change at master point location \mathbf{u}_m ; d_m is the distance between the master point location \mathbf{u}_m and the well with the index w ; ω is the exponent that offers considerable flexibility of the formula similar as that used in the inverse distance method^[14]. Different choices of the exponent ω will result in different estimates. For progressively larger values of ω the closest sample would receive a progressively larger percentage of the total weight. The choice of ω is arbitrary. c is a tolerance with a small value.

The new pressure and production rates can be calculated from a linearization formula by assuming the independent changes of the properties at master point locations:

$$\begin{aligned}
p_{w,t}^{opt} &= p_{w,t}^i + \sum_{m=1}^{n_m} \{ SP_{\phi,m,w,t}^i \Delta\phi(\mathbf{u}_m) \} \\
&+ \sum_{m=1}^{n_m} \{ SP_{K_h,m,w,t}^i \Delta K_h(\mathbf{u}_m) \} \\
&+ \sum_{m=1}^{n_m} \{ SP_{K_v,m,w,t}^i \Delta K_v(\mathbf{u}_m) \}
\end{aligned} \tag{34}$$

for all pressure observations

$$\begin{aligned}
q_{w,t}^{opt} &= q_{w,t}^i + \sum_{m=1}^{n_m} \{ SQ_{\phi,m,w,t}^i \Delta\phi(\mathbf{u}_m) \} \\
&+ \sum_{m=1}^{n_m} \{ SQ_{K_h,m,w,t}^i \Delta K_h(\mathbf{u}_m) \} \\
&+ \sum_{m=1}^{n_m} \{ SQ_{K_v,m,w,t}^i \Delta K_v(\mathbf{u}_m) \}
\end{aligned} \tag{35}$$

for all fractional flow rate observations

The objective function, global mismatch of the reservoir, can be calculated by:

$$\begin{aligned}
\Delta^{2opt} &= w_p \left(\frac{\Delta^{2opt}_P}{2} \right) + w_q \left(\frac{\Delta^{2opt}_Q}{2} \right) \\
&= \frac{W_p}{2\Delta P^0} \left\{ \sum_{w=1}^{n_w} \left\{ \sum_{t=1}^{n_{w,p}} (p_{w,t}^{opt} - p_{w,t})^2 \lambda_{w,p,t} \right\} \beta_w \right. \\
&\quad \left. - \sum_{w=1}^{n_w} \left\{ \sum_{t=1}^{n_{w,p}} (p_{w,t}^0 - p_{w,t})^2 \lambda_{w,p,t} \right\} \beta_w \right\} \\
&+ \frac{W_q}{2\Delta Q^0} \left\{ \sum_{w=1}^{n_w} \left\{ \sum_{t=1}^{n_{w,q}} (q_{w,t}^{opt} - q_{w,t})^2 \lambda_{w,q,t} \right\} \beta_w \right. \\
&\quad \left. - \sum_{w=1}^{n_w} \left\{ \sum_{t=1}^{n_{w,q}} (q_{w,t}^0 - q_{w,t})^2 \lambda_{w,q,t} \right\} \beta_w \right\}
\end{aligned} \tag{36}$$

When the property changes at one master point location are considered independently, e.g., $\Delta K_h(\mathbf{u}_m)$ and $\Delta K_v(\mathbf{u}_m)$ are thought as zeros when $\Delta\phi(\mathbf{u}_m)$ is considered:

$$p_{w,t,\phi}^{opt} = p_{w,t}^i + SP_{\phi,m,w,t}^i \Delta\phi(\mathbf{u}_m) \tag{37}$$

$$q_{w,t,\phi}^{opt} = q_{w,t}^i + SQ_{\phi,m,w,t}^i \Delta\phi(\mathbf{u}_m) \tag{38}$$

for $m=1, 2, \dots, n_m$ and all observation values

The objective function is obtained by substituting $p_{w,t}^{opt}$ and $q_{w,t}^{opt}$ in Equation (36) by $p_{w,t,\phi}^{opt}$, $q_{w,t,\phi}^{opt}$ from Equations (37) and (38). By minimizing the objective function the optimal perturbations of property at all master point locations can be obtained:

$$\Delta\phi^*(\mathbf{u}_m), \text{ for } m=1, 2, \dots, n_m$$

By same procedure, based on the formulas:

$$p_{w,t,K_h}^{opt} = p_{w,t}^i + SP_{K_h,m,w,t}^i \Delta K_h(\mathbf{u}_m) \quad (39)$$

$$q_{w,t,K_h}^{opt} = q_{w,t}^i + SQ_{K_h,m,w,t}^i \Delta K_h(\mathbf{u}_m) \quad (40)$$

$$p_{w,t,K_v}^{opt} = p_{w,t}^i + SP_{K_v,m,w,t}^i \Delta K_v(\mathbf{u}_m) \quad (41)$$

$$q_{w,t,K_v}^{opt} = q_{w,t}^i + SQ_{K_v,m,w,t}^i \Delta K_v(\mathbf{u}_m) \quad (42)$$

for $m=1, 2, \dots, n_m$ and all observation values

The optimal perturbation values of permeability at all master point locations can be obtained:

$$\Delta K_h^*(\mathbf{u}_m), \Delta K_v^*(\mathbf{u}_m), \text{ for } m=1, 2, \dots, n_m$$

Optimal values, $\Delta\phi^*(\mathbf{u}_m)$, $\Delta K_h^*(\mathbf{u}_m)$ and $\Delta K_v^*(\mathbf{u}_m)$, can be converted into the optimal factors:

$$f_\phi^*(\mathbf{u}_m) = \frac{\phi^i(\mathbf{u}_m) + \Delta\phi^*(\mathbf{u}_m)}{\phi^i(\mathbf{u}_m)} \quad (43)$$

$$f_{K_h}^*(\mathbf{u}_m) = \frac{K_h^i(\mathbf{u}_m) + \Delta K_h^*(\mathbf{u}_m)}{K_h^i(\mathbf{u}_m)} \quad (44)$$

$$f_{K_v}^*(\mathbf{u}_m) = \frac{K_v^i(\mathbf{u}_m) + \Delta K_v^*(\mathbf{u}_m)}{K_v^i(\mathbf{u}_m)} \quad (45)$$

for $m=1, 2, \dots, n_m$

Step 7: Creation of a New Set of Porosity and Permeability for the New Iteration

The factors for all grid nodes are generated by kriging using the n_m known factors from optimization at master point locations from Step 6:

$$f_\phi^*(\mathbf{u}_g), f_{K_h}^*(\mathbf{u}_g), f_{K_v}^*(\mathbf{u}_g)$$

for $g=1, 2, \dots, N$

The factors will change between iterations. Then models of porosity and permeability for the next iteration are calculated by:

$$\phi^{i+1}(\mathbf{u}_g) = \phi^i(\mathbf{u}_g) \cdot f_\phi^*(\mathbf{u}_g) \quad (46)$$

$$K_h^{i+1}(\mathbf{u}_g) = K_h^i(\mathbf{u}_g) \cdot f_{K_h}^*(\mathbf{u}_g) \quad (47)$$

$$K_v^{i+1}(\mathbf{u}_g) = K_v^i(\mathbf{u}_g) \cdot f_{K_v}^*(\mathbf{u}_g) \quad (48)$$

for $g=1, 2, \dots, N$

Step 8: Rerun Flow Simulation with the Updated Property Model

A flow simulation is executed with the property models obtained from Equations (46), (47) and (48) and the new simulation results of well bottom-hole pressure and fractional flow rates at all well locations are obtained:

$$P_{w,t}^{i+1} \quad \text{for } w=1, 2, \dots, n_w \text{ and } t=1, 2, \dots, n_{w,p}$$
$$q_{w,t}^{i+1} \quad \text{for } w=1, 2, \dots, n_w \text{ and } t=1, 2, \dots, n_{w,q}$$

Step 9: Calculation of the Mismatch of the Updated Models

The mismatch in pressure and fractional flow rates as well as the global mismatch are calculated. If the global mismatch of reservoir or the mismatch at any well is larger than a specified tolerance, go back to Step 3 until the global mismatch and the mismatch at all wells are small enough or cannot be improved.

Some Other Implementation Aspects

The base model should be a geostatistical realization conditional to all available core /well logs, trends and seismic data. The fractional flow rate in the methodology may be different for different well control options in flow simulation. For the case of liquid rate control, oil production rate can be selected as the fractional flow rate.

The perturbation locations should be set near the wells with high mismatch and can simply be set to the well locations. The average properties in the grid blocks containing the wells may not be equal to the values at well locations. The general principle is to select the location with the highest mismatch as the perturbation location.

The perturbation factor values at the selected perturbation locations have little effect on the final convergence level of the results. The range of perturbation should not be too large or too small for the local updating: half to one and a half well space showed to be quite adequate for the cases investigated in this work. The weights, β_w , $\lambda_{w,p,t}$ and $\lambda_{w,q,t}$, can be set to any suitable values in order to take account for the accuracy and relative importance of the various different observed data points.

Using information from earlier runs is the most efficient method to compute the sensitivity coefficients. There is a “base case” run and a “sensitivity” run at each iteration. The “base case” run is a plausible reservoir model. The “sensitivity” run has reservoir properties that have been unnaturally altered for the purposes of sensitivity coefficient calculation.

This methodology assumes that the all parameter settings except property models are reliable and tries to create the porosity and permeability models with the lowest mismatch between the observed data and simulation results. Therefore, this methodology may not get a perfect match between the observed data and the simulation results, especially for well bottom-hole pressure. With the reservoir model created by the proposed method, changing well production index, skin factor or transmissibility factor suitably can reduce mismatch in pressure and global mismatch considering that well conditions may be changed by a stimulation operation.

Conclusions

We propose a new method to integrate production data into reservoir models by the local updating of porosity and permeability fields. This method is aimed at understanding the static changes in porosity and permeability that are required to better match historical production data; the method is intended for production data integration. The method could also be used in automatic history matching mode, where the main goal is to match history by changing a variety of parameters including dynamic flow parameters.

This method focuses on post processing an initial model to injection/production rate and pressure history by an iterative scheme with simultaneously calculated numerical sensitivity coefficients. One or multiple perturbation locations are selected based on the mismatch at each well. The selected master point locations are defined and used as reference positions to calculate the sensitivity coefficients of well bottom hole pressure and flow rate subject to changes in porosity and permeability. The optimal changes of porosity and permeability at the master point locations are obtained by minimizing the objective function related to reservoir responses of pressure and fractional flow rate calculated by a linearized formula for flow simulation based on porosity and permeability changes. The optimized changes are propagated to the entire grid system by kriging. Integrating flow simulation and kriging algorithms within an optimization process and calculating sensitivity coefficients numerically at the same time constitute the proposed methodology.

This method makes it possible to condition permeability/porosity realizations to production rate and pressure history data simultaneously.

Nomenclature

f	=	factor of property change, dimensionless
G	=	index of grid blocks in grid system
h	=	thickness
i_s	=	index of perturbation grid block , $i_s \in 1, 2, \dots, N$
K	=	permeability
\bar{k}	=	average permeability
$K_h(\mathbf{u}_g)$	=	horizontal permeability at the location \mathbf{u}_g
$\hat{K}_h(\mathbf{u}_g)$	=	horizontal permeability at the location \mathbf{u}_g in the perturbed model
$K_v(\mathbf{u}_g)$	=	vertical permeability at the location \mathbf{u}_g
$\hat{K}_v(\mathbf{u}_g)$	=	vertical permeability at the location \mathbf{u}_g in the perturbed model
M	=	index of master point locations, $m = 1, 2, \dots, n_m$
N	=	number of cells in grid system
n_m	=	number of master point locations
n_p	=	number of the available observed pressure data
n'_p	=	number of the well bottom hole pressure from simulation
n_q	=	number of the available observed fractional flow rate data
n'_q	=	number of the quarterly averaged well oil production rates from simulation
n_s	=	number of perturbation locations
n_w	=	number of wells
$n_{w,p}$	=	number of available observed pressure data for the well with the index w
$n_{w,q}$	=	number of available observed fractional flow rate data for the well with the index w
p_w	=	pressure at the well with the index w
$p_{w,t}$	=	the t th observed well bottom-hole pressure datum at the well with the index w
$p_{w,t,m}$	=	the t th well bottom pressure datum at the well with the index w after introducing perturbation at location \mathbf{u}_m
\hat{p}	=	pressure from flow simulation with the perturbed model
$q_{w,t}$	=	observed fractional flow rate
$q_{w,t,m}$	=	fractional flow rate at the well with the index w after introducing perturbation at location \mathbf{u}_m
\hat{q}	=	fractional flow rate from simulation with the perturbed model
s	=	index of perturbation locations
SP	=	sensitivity coefficients of well bottom hole pressure
SQ	=	sensitivity coefficients of fractional flow rate
t	=	index of the time corresponding to the observed data
\mathbf{u}	=	location

w	=	well index
w_p	=	weight of mismatch in pressure, dimensionless
w_q	=	weight of mismatch in fractional flow rate, dimensionless
β_w	=	the weight for the data at the well with the index w , dimensionless
$\phi(\mathbf{u}_g)$	=	porosity at the location \mathbf{u}_g , dimensionless
$\hat{\phi}(\mathbf{u}_g)$	=	porosity at the location \mathbf{u}_g in the perturbation model, dimensionless
$\lambda_{w,p,t}$	=	weight for the t th observed pressure data at the well with the index w , dimensionless
$\lambda_{w,q,t}$	=	weight for the t th observed fractional flow rate measured at the well with the index w , dimensionless
$\Delta\hat{\phi}(\mathbf{u}_g)$	=	change of porosity at the location \mathbf{u}_g for the perturbed model, dimensionless
$\Delta\hat{k}_h(\mathbf{u}_g)$	=	change of horizontal permeability at the location \mathbf{u}_g for the perturbed model
$\Delta\hat{k}_v(\mathbf{u}_g)$	=	change of vertical permeability at the location \mathbf{u}_g for the perturbed model
$\Delta p_{w,t,m}$	=	pressure difference at the well with the index w introduced by the perturbation at the location \mathbf{u}_m
$\Delta p_{w,t,total}$	=	pressure difference at the well with the index w introduced by joint perturbations
ΔP	=	pressure mismatch of reservoir
ΔP_w	=	pressure mismatch at the well with the index w
$\Delta q_{w,t,m}$	=	difference of fractional flow rate at the well with the index w introduced by the perturbation at location \mathbf{u}_m
$\Delta q_{w,t,total}$	=	difference of fractional flow rate at the well with the index w introduced by joint perturbations
ΔQ	=	mismatch in fractional flow rate of reservoir
ΔQ_w	=	mismatch in fractional flow rate at the well with the index w
Δ	=	global mismatch of reservoir, dimensionless
Δ_w	=	global mismatch at the well with index w , dimensionless
Δ^2	=	change in global mismatch for reservoir, dimensionless
Δ_P^2	=	change of pressure mismatch of reservoir, dimensionless
Δ_Q^2	=	change of mismatch in fractional flow rate of reservoir, dimensionless

Superscripts

0	=	base model
i	=	iteration number
opt	=	calculated by sensitivity coefficients
*	=	optimal values corresponding to the lowest mismatch calculated by the linearized formula with sensitivity coefficients

References

1. C. V. Deutsch, *Geostatistical Reservoir Modeling*; *Oxford University Press, New York (2002)*, 376 pages.
2. L.B. Cunha, D.S. Oliver, R.A. Redner, and A.C. Reynolds, A Hybrid Markov Chain Monte Carlo method for generating permeability fields conditioned to multiwell pressure data and prior information; *SPE 36566 presented at the 1996 SPE Annual Technical conference and exhibition, Denver, Oct. 6-9.*
3. X. H. Wen, C. V. Deutsch, and A.S. Cullick, High-resolution reservoir models integrating multiple well production data; *SPEJ*, pp 344-355, 1998.
4. X. H. Wen, T. T. Tran, and R. A. Behrens and J. J. Gomez-Hernandez, Production data integration in sand/shale reservoirs using sequential self-calibration and GeoMorphing: A comparison; *SPEJ*, pp 255-265, 2002.
5. H. Qassab, M. Khalifa, N. Afaleg, and H. Ali, Streamline-based production data integration under realistic field conditions: Experience in a giant middle-eastern reservoir; *SPE 84079 presented at the 2003 SPE Annual Technical conference and exhibition, Denver, Oct. 5-8.*
6. B. Agarwal, and B. Martin, A streamline-based method for assisted history matching applied to an Arabian Gulf Field; *SPE 84462 presented at the 2003 SPE Annual Technical conference and exhibition, Denver, Oct. 5-8.*
7. K. Tarun, and S. Srinivasan, Iterative integration of dynamic data in reservoir models; *SPE 84592 presented at the 2003 SPE Annual Technical conference and exhibition, Denver, Oct. 5-8.*
8. L.Y. Hu, Combination of Dependent Realizations within the gradual deformation method; *Mathematical Geology*, pp 953-964, 2002.
9. M. Feraille, F. Roggero, E. Manceau, L.Y. Hu, I.Zabalza-Mezghani, and L. Costa Reis, Application of Advanced history matching techniques to an integrated field cases; *SPE 84463 presented at the 2003 SPE Annual Technical conference and exhibition, Denver, Oct. 5-8.*
10. P. C. Shah, G. R. Gavalas, and J. H. Seinfeld, Error Analysis in History Matching: The Optimum Level of Parametrization; *SPEJ*, pp 219-228, Jun. 1978.
11. A.S. Emanuel', R.W. Tang, D.M. McKay, and M.H. Ellis, A Hybrid Simulation Study of the Vindalia Sand Waterflood; *SPE 26477 presented at the 1993 SPE Annual Technical conference and exhibition, Houston, Oct.3-6.*
12. Peter H. Sammon, A Nine-Point Differencing scheme Based on High order Stream Tube Modeling; *SPE 21223 presented at the 1991 SPE Annual Technical conference and exhibition, Ansheim, Feb.17-20.*
13. GeoQuest/Schlumberger; *ECLIPSE User's Manual Version 2003.*
14. Edward H. Isaaks, and R. Mohan Srivastava, *Applied Geostatistics*; *Oxford University Press, New York (1989)*, 561 pages.

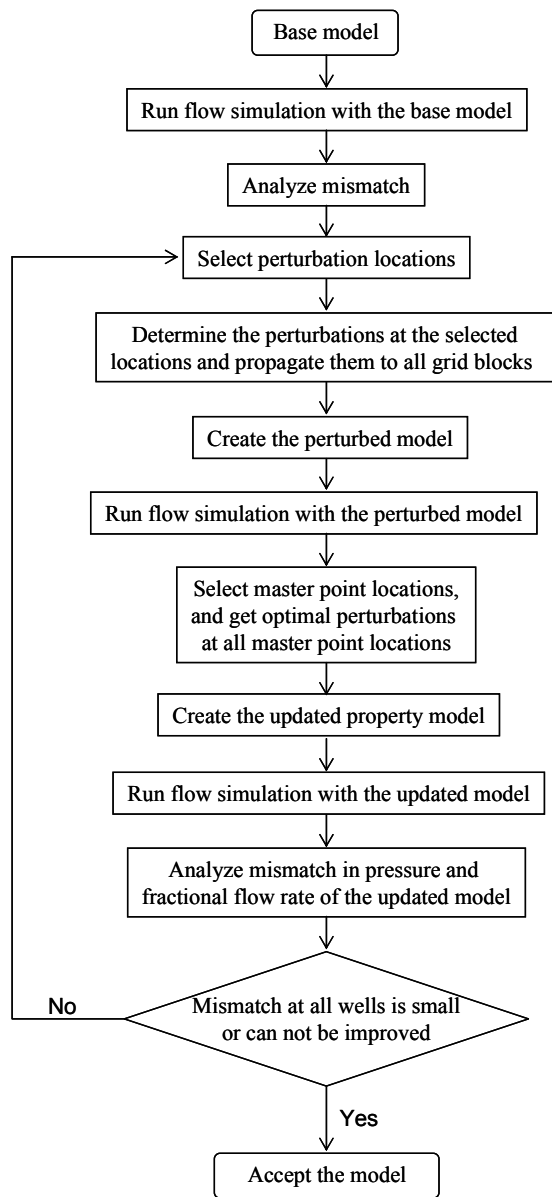


Figure 1. Schematic procedure of the proposed methodology.

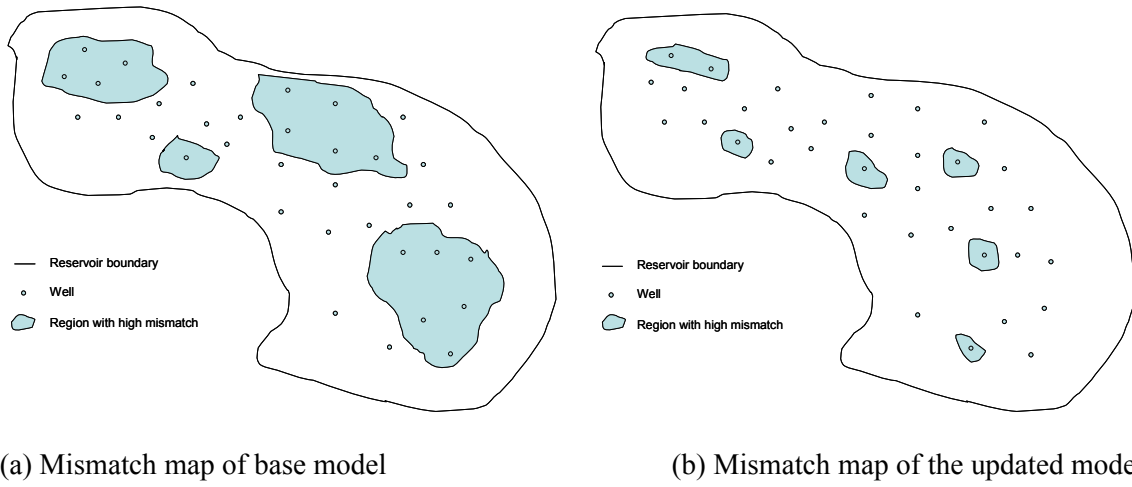


Figure 2. Mismatch maps of the base model and the updated model.

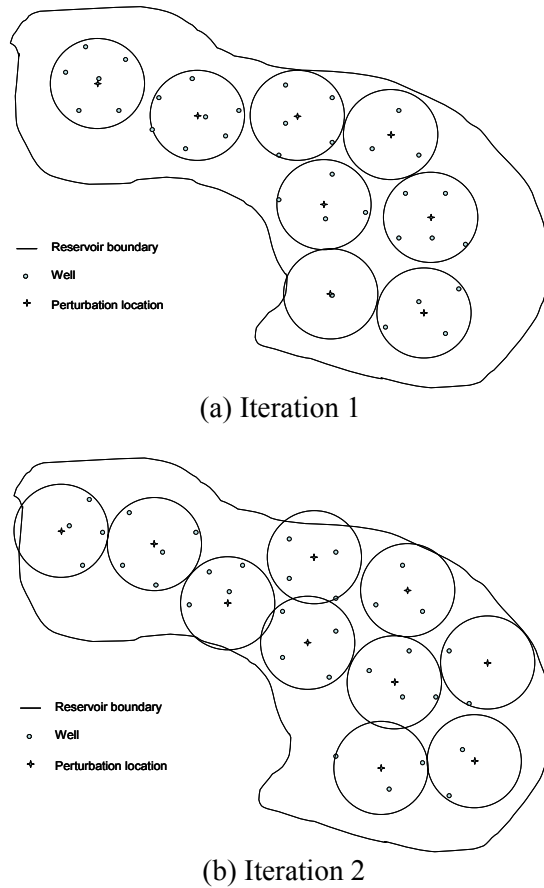


Figure 3: A schematic plot that illustrates different perturbation locations between iterations.

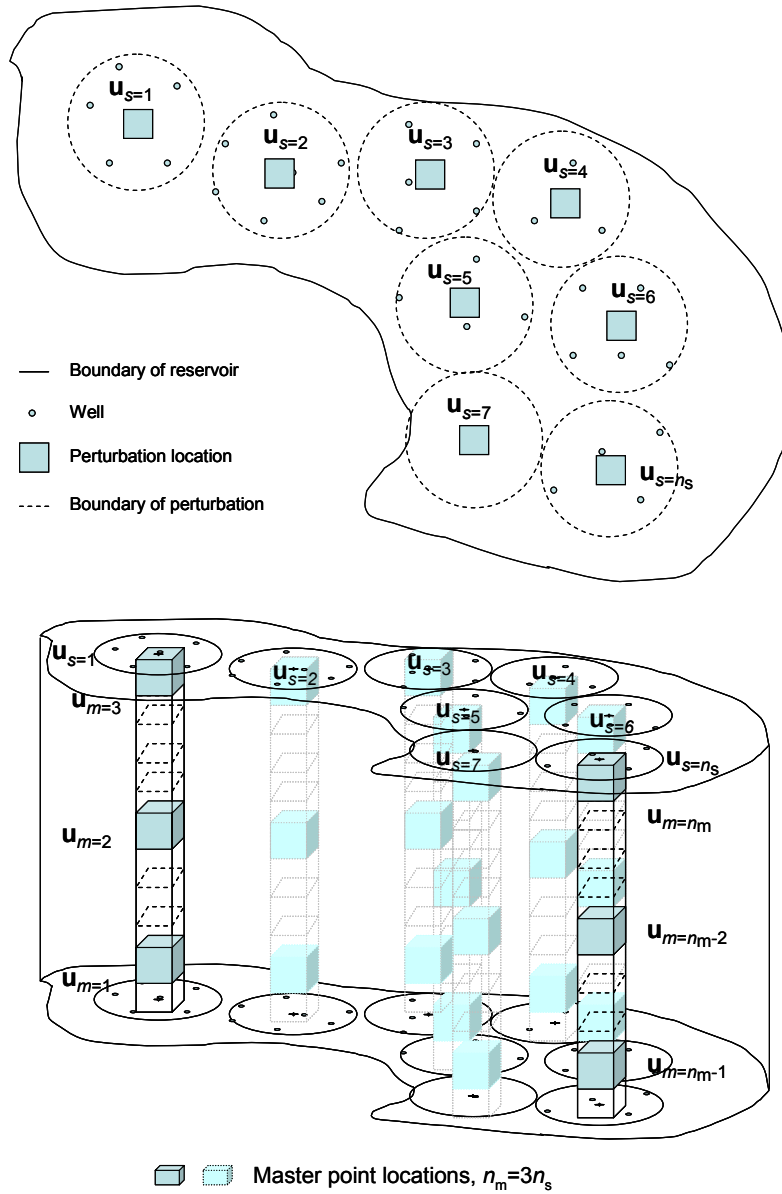


Figure 4. Illustration of perturbation locations and master point locations.